

Journal of Biomaterials Applications

<http://jba.sagepub.com/>

Structural and cellular characterization of electrospun recombinant human tropoelastin biomaterials

Kathryn A McKenna, Kenton W Gregory, Rebecca C Sarao, Cheryl L Maslen, Robert W Glanville and Monica T Hinds

J Biomater Appl 2012 27: 219 originally published online 17 May 2011

DOI: 10.1177/0885328211399480

The online version of this article can be found at:
<http://jba.sagepub.com/content/27/2/219>

Published by:



<http://www.sagepublications.com>

Additional services and information for *Journal of Biomaterials Applications* can be found at:

Email Alerts: <http://jba.sagepub.com/cgi/alerts>

Subscriptions: <http://jba.sagepub.com/subscriptions>

Reprints: <http://www.sagepub.com/journalsReprints.nav>

Permissions: <http://www.sagepub.com/journalsPermissions.nav>

Citations: <http://jba.sagepub.com/content/27/2/219.refs.html>

>> [Version of Record](#) - Jul 26, 2012

[OnlineFirst Version of Record](#) - May 17, 2011

[What is This?](#)

Structural and cellular characterization of electrospun recombinant human tropoelastin biomaterials

Kathryn A McKenna^{1,2}, Kenton W Gregory¹, Rebecca C Sarao¹, Cheryl L Maslen³, Robert W Glanville¹ and Monica T Hinds²

Abstract

An off-the-shelf vascular graft biomaterial for vascular bypass surgeries is an unmet clinical need. The vascular biomaterial must support cell growth, be non-thrombogenic, minimize intimal hyperplasia, match the structural properties of native vessels, and allow for regeneration of arterial tissue. Electrospun recombinant human tropoelastin (rTE) as a medial component of a vascular graft scaffold was investigated in this study by evaluating its structural properties, as well as its ability to support primary smooth muscle cell adhesion and growth. rTE solutions of 9, 15, and 20 wt% were electrospun into sheets with average fiber diameters of 167 ± 32 , 522 ± 67 , and 735 ± 270 nm, and average pore sizes of 0.4 ± 0.1 , 5.8 ± 4.3 , and 4.9 ± 2.4 μm , respectively. Electrospun rTE fibers were cross-linked with disuccinimidyl suberate to produce an insoluble fibrous polymeric recombinant tropoelastin (prTE) biomaterial. Smooth muscle cells attached via integrin binding to the rTE coatings and proliferated on prTE biomaterials at a comparable rate to growth on prTE coated glass, glass alone, and tissue culture plastic. Electrospun tropoelastin demonstrated the cell compatibility and design flexibility required of a graft biomaterial for vascular applications.

Keywords

elastin, cell adhesion, cell proliferation, vascular biomaterial, tissue engineering

Introduction

Cardiovascular disease remains one of the leading causes of morbidity and mortality in the Western world, affecting nearly 81 million people in the United States alone in 2006.¹ Treatment options for bypass grafts are limited to either autologous vessels, which are often not available and can be affected by pre-existing disease, or synthetic grafts, which are limited to vessels larger than 6 mm in diameter.² Small diameter vascular grafts have been under development for more than 50 years with limited clinical success. Vascular grafts often fail due to thrombosis, intimal hyperplasia, and aneurysm formation.³

To address the failure of small diameter vascular grafts, tissue engineered vascular grafts have been extensively studied using both synthetic and natural biomaterial scaffolds. Synthetic scaffolds, including ePTFE, poly(ethylene glycol) diacrylate, poly(caprolactone), and polyurethane, have the advantages of controllable structural and mechanical properties

while being highly reproducible and easily manufactured in large scale quantities. Yet these synthetic scaffolds typically lack the elasticity of native arterial walls and the biocompatibility for long term vascular cell functionality. Natural biomaterial scaffolds, including the most studied grafts of decellularized arteries, have also had limited success. The two most successful examples of decellularized arteries without cell seeding have

¹Oregon Medical Laser Center, Providence St. Vincent Medical Center, 9205 SW Barnes Road, Portland, Oregon, 97225, USA

²Department of Biomedical Engineering, Oregon Health & Science University, 3303 SW Bond Avenue, Mailcode: CH13B, Portland, Oregon, 97239, USA

³Division of Cardiovascular Medicine, Oregon Health & Science University, 3303 SW Bond Avenue, Mailcode: CH14B, Portland, Oregon, 97239, USA

Corresponding author:

Monica T Hinds, Department of Biomedical Engineering, Oregon Health & Science University, 3303 SW Bond Avenue, Mailcode: CH13B, Portland OR 97239, USA
 Email: hindsm@ohsu.edu

been Sawyer's ficin-digested glutaraldehyde-tanned bovine carotid graft⁴ and Dardik's glutaraldehyde-tanned human umbilical vein graft.⁵ While the 5-year patency rates were promising, aneurysm formation due to *in vivo* degradation limited their widespread use.^{5,6} Decellularized arteries are attractive scaffolds for tissue-engineered vascular grafts due to their mechanical and biological properties,⁷ yet these natural scaffolds are still limited by the lack of precise manufacturing control of their structural properties.

Tissue-engineered vascular grafts which are produced from autologous cells without a scaffold have recently advanced from the research bench to clinical safety trials using an arteriovenous shunt model, with 10 reported patients.^{8,9} These tissue-engineered grafts have shown promising results with primary patency rates of 78% at 1 month and 60% at 6 months with failures due to thrombosis, dilation, and aneurysm, but their lengthy production times of 24 weeks⁸ will be a limiting factor in becoming a practical clinical option. Small diameter tissue-engineered vascular graft development has been the focus of many research groups, but a viable option that structurally compares to native arteries, supports cell growth, and is functionally equivalent to autografts, the gold standard treatment option, has not been found.

Electrospinning suspensions of monomers or polymers from both natural proteins and synthetic polymers can produce sub-micron sized fibers, which can then be cross-linked to produce stable polymeric structures.^{10,11} The structural properties of the electrospun fibers, primarily fiber shape and diameter, can be controlled by varying the gap distance, accelerating voltage, solution viscosity, and solution delivery rate.^{10,12} Adding this degree of control to a natural protein such as elastin is clearly advantageous. Elastin is a key extracellular matrix protein responsible for energy storage and recovery in native elastic arteries.¹³ End stage aneurysm disease and supravalvular aortic stenosis have been associated with the lack of elastin and deficiency in elastin expression.^{14–20} Therefore, elastin has been proposed as an essential component in vascular graft design.^{21,22} Elastin has been electrospun for use in tissue-engineered grafts,^{12,23–28} but the elastin protein has primarily been extracted from assembled and cross-linked animal-sourced tissues. These forms of elastin may maintain critical elastin biochemical signaling, but are likely to elicit an immuno-rejection response leading to graft degradation and ultimate aneurismal graft failure. The electrospinning of human tropoelastin, the monomer unit of elastin, is promising^{27,29} as a medial component of tissue engineered vascular grafts, but the limited analysis of the effects of cross-linking as well as the interactions with vascular cells, necessitates further study.

In this study, we created an electrospun biomaterial entirely from recombinant human tropoelastin (rTE) and used a unique cross-linker to create fibrous polymeric recombinant tropoelastin (prTE) that mimics the structural properties of native elastin fibers and supports vascular cell adhesion and growth. This unique biomaterial can be a scaffold for vascular tissue engineering applications with customizable dimensions in terms of both individual fiber size and gross graft dimensions.

Materials and methods

Materials

A codon optimized synthetic gene for human tropoelastin was expressed in gram quantities in a 10 L *E.coli* fermentation system. The expression construct includes all of the functional exons except exon 1, which encodes the signal sequence, exon 22 and exon 26A, which are rarely if ever expressed in natural elastin. This produces an elastin isoform that is the same as one of the natural isoforms produced by normal human cells. The purification procedure resulted in a >99% pure product as determined by gel electrophoresis. Control materials of extracted elastin were obtained using a hot alkali digestion method on native carotid arteries from domestic swine (Animal Technologies, Tyler, TX).^{30,31} All chemical reagents were acquired from Sigma-Aldrich unless otherwise noted.

Electrospinning of rTE

A 2 mL glass syringe was loaded with 9, 15, or 20 wt% rTE in 1,1,1,3,3-hexafluoro-2-propanol (HFP). An 18-gage stainless steel blunt tip needle was connected to the glass syringe and loaded onto a syringe pump (Harvard Apparatus). A high voltage power supply (Glassman High Voltage, Inc., High Bridge, NJ) was electrically coupled to the end of the needle. A gap distance of 12.5 cm was set from the end of the needle to the center of the collection device. Fibers were spun onto grounded collection devices of either copper foil covered plates for fiber analysis or Poly-D-Lysine coated coverslips (Fisher) attached to copper foil covered plates for cell studies. Mandrels rotated at 4000–6000 rpm and translated longitudinally 6–8 cm with a rate of 8 cm/s on a custom-built device for electrospun tube formation. The solution was charged at 18.5 kV with the high voltage power supply. The syringe pump advanced the protein solution at 2 mL/h. All electrospinning was conducted within a fume hood.

Cross-linking of electrospun rTE

All samples of electrospun rTE were cross-linked using the organic cross-linker disuccinimidyl suberate (DSS), (Pierce Biotechnology-Thermo Fisher Scientific Inc.) to produce the polymer, prTE. Samples were cross-linked in a two-stage process. The electrospun rTE samples were incubated for 4 h in DSS, in 50 mL anhydrous ethyl acetate, at a ratio of 0.072 mg of DSS per mg of rTE protein at room temperature. A second incubation occurred for 12–18 h at a concentration of 0.108 mg of DSS per mg of rTE protein at room temperature. prTE samples were then rinsed in anhydrous ethyl acetate for 5 min with a second 5 min rinse in 70% ethanol, and a final 10 min rinse in deionized water. The final product was stored in 70% ethanol.

Electrospun rTE fiber characterization

Electron microscopy was used to determine the electrospinning consistency, fiber characterization, and to evaluate the internal nanostructure of electrospun fibers. rTE solutions were electrospun onto copper foil covered plates. Electrospun rTE and prTE samples were mounted onto scanning electron microscopy (SEM) stubs and sputter-coated with 250 Å of gold/palladium. Micrographs were taken at magnifications from 1000 to 10,000 \times and viewed at 5–30 kV on either a Zeiss Model 960 Analytical SEM or a FEI Sirion XL30 SEM. For transmission electron microscopy (TEM) analysis the electrospun rTE samples were adhered to copper TEM slot grids using silver paint. Carbon (~200 Å) was coated onto both sides of the sample on TEM grids using an evaporation coater. Samples were viewed with a JOEL Model 2000fx Analytical TEM/Scanning TEM at 200 kV.

The fiber diameters and pore sizes of rTE flat materials were measured from SEM micrographs using ImageJ software (NIH). Twenty measurements were taken for each picture with three pictures analyzed per electrospinning run. Five separate lots of rTE were analyzed for the 15 wt% rTE samples. Matlab analysis was used to determine the degree of fiber orientation.³²

Smooth muscle cell adhesion to adsorbed rTE

Baboon carotid artery smooth muscle cells (SMCs) were isolated³³ and used to assess the adhesion of vascular cells on adsorbed rTE. SMCs were maintained in a media consisting of minimum essential media (MEM), 10% Fetal Bovine Serum (FBS), 5 mM L-glutamine, and a 1% penicillin, streptomycin,

and fungizone mix (Invitrogen). SMCs were maintained and passaged in culture using standard techniques. For all adhesion assays, the SMCs were plated in adhesion media (MEM with 1 mg/mL of BSA).

To determine the optimal rTE concentration for SMC adhesion, rTE solutions from 0 to 5 mg/mL in PBS were prepared and added to 12 wells of a 96-well plate. Plates were sealed and incubated at 4°C overnight. Plates were then rinsed twice with PBS and seeded with 2×10^4 SMCs per well and incubated at 37°C for 90 min. Plates were then rinsed twice to remove loosely adhered and nonadherent cells and subsequently frozen at –80°C. Cell numbers were then evaluated using the CyQUANT® GR assay (Invitrogen). Fluorescence units were converted to cell numbers using standard curves generated from known cell numbers. Studies were repeated three times.

The adhesion mechanisms of SMCs to adsorbed rTE were determined and compared to SMC adhesion to adsorbed coatings of fibronectin and collagen, as well as uncoated tissue-culture treated plastic (TCP). 96-well plates were coated with 50 µg/mL of each protein overnight at 4°C. Plates were rinsed with PBS and incubated for 1 h with 10 mg/mL BSA in PBS. Cells were removed gently from flasks with Versene (2% EDTA in PBS) and 0.05% Trypsin. Trypsin was deactivated following cell removal with 0.5 mg/mL soybean trypsin inhibitor. Plates were rinsed with PBS and SMCs were subsequently seeded at 2×10^4 cells per well on each substrate in each of the following media: adhesion media, adhesion media supplemented with EDTA (5 mM), pertussis toxin (0.5 µg/mL), or lactose (5 mM). Cells were incubated at 37°C for 90 min. Plates were then rinsed to remove loosely adherent cells with PBS and frozen at –80°C for subsequent analysis with CyQUANT® GR. Studies were run in 10 wells per condition and repeated three times.

Smooth muscle cell growth on electrospun prTE

Growth curves were constructed for SMCs grown on TCP coverslips as well as Poly-D-Lysine glass coverslips that were either untreated, coated with prTE, or electrospun with prTE. Three separate lots of rTE were tested with a sample size of 6 per condition. prTE samples were electrospun from 15 wt% rTE solutions onto Poly-D-Lysine coated glass coverslips and cross-linked. prTE fibers were fluorescently stained with 2.5 µg/mL Oregon Green® 488-X, succinimidyl ester *6-isomer* (Invitrogen) for 1 h at room temperature. Coated prTE coverslips were prepared by adding 0.2 wt% rTE solutions in HFP onto 12 mm diameter Poly-D-Lysine coverslips. Samples were air-dried,

cross-linked, and soaked in 70% ethanol overnight. prTE samples were rinsed twice for 5 min with PBS and then incubated for 20 min in media.

SMCs (5×10^3 cells/cm 2) were seeded onto cover-slips and evaluated at 1, 2, 3, 5, and 7 days. Media was replaced at each timepoint with 500 μ L of a 10% alamarBlue® solution (Invitrogen) in media and incubated at 37°C for 2 h. 200 μ L of the reduced alamarBlue® solution was removed from each well and transferred to a 96-well plate for immediate analysis on a SPECTRAFluor Plus plate reader (TECAN) at an excitation wavelength of 560 nm and an emission wavelength of 590 nm at 37°C. Any remaining alamarBlue® solution was aspirated from the wells and 500 μ L fresh SMC media was added to each well. Measurements were normalized to the 24 h timepoint for each condition. Doubling times of metabolic activity were calculated as $(t_2 - t_1)/(\log(\text{AB fluorescence at } t_2) - \log(\text{AB fluorescence at } t_1)) * 3.32$, where $t_2 = 120$ h and $t_1 = 72$ h.

At day 8 a CyQUANT® NF cell proliferation assay (Invitrogen) was performed. Media was removed from the wells and 500 μ L 1X dye binding solution, which consisted of 2 μ L of dye reagent per mL of Hank's balance salt solution (HBSS) buffer, was added to each well. The plates were covered and incubated for 1 h at 37°C. 200 μ L of the dye solution was then transferred to a 96-well plate for immediate analysis on a SPECTRAFluor Plus plate reader with an excitation wavelength of 485 nm and an emission wavelength of 535 nm at 37°C. Measurements for each surface were normalized to the TCP condition.

Cell attachment and spreading were evaluated at 24 and 48 h post seeding. SMCs (2×10^3 cells/cm 2) were seeded onto electrospun prTE samples prepared in the same manner as the growth curves. Cells were fixed at each timepoint with 2.5% paraformaldehyde for 1 h at room temperature. SMCs were permeabilized with 0.1% Triton-X 100 for 5 min and subsequently stained with rhodamine phalloidin (1 unit/sample) and 300 nM DAPI (Invitrogen) to visualize the cytoskeleton and nuclear structures. Confocal images were taken with a 63X oil objective on a Zeiss Multiphoton Confocal microscope using 488, 543, and 780 nm excitation wavelengths.

Statistical analyses

All data are expressed as the mean \pm standard deviation. Student's *t*-test, linear regression, and one-way ANOVA with Tukey's *post hoc* test were used for hypothesis testing, with $p < 0.05$ as the measure for statistical significance. The number of independent tests is listed for each experiment.

Results

Morphology and substructure of rTE and prTE fibers

Human tropoelastin was successfully electrospun onto flat collection plates at concentrations of 9, 15, and 20 wt% rTE (Figure 1) to produce fibrous sheets, which were comparable in structure to extracted porcine elastin (Figure 2). The average fiber diameter was dependent on the rTE concentration (Table 1). For each concentration of rTE, the electrospun fiber diameters were consistent with no statistical differences between production lots (ANOVA, $p = 0.16$). Extracted porcine carotid elastin had an average fiber diameter of 870 nm, which was larger and more variable (323–1843 nm) than the electrospun samples. The fiber sizes were significantly different from the native extracted elastin for the 9 wt% (Tukey, $p < 0.01$) and 15 wt% solutions (Tukey, $p < 0.01$), but not significantly different from the 20 wt% solution (Tukey, $p = 0.32$). While the gross morphology of the 9 and 15 wt% fibers was rounded, many of the rTE fibers spun from 20 wt% solutions were ribboned and contained voids within their fibers (Figure 3).

The pore sizes of the electrospun rTE scaffolds were quantified and compared to native elastin. The electrospun 15 and 20 wt% rTE had pore sizes of 5.8 ± 4.3 μ m 2 and 4.9 ± 2.4 μ m 2 , respectively, which is similar to the native elastin with 3.7 ± 1.6 μ m 2 (ANOVA, Tukey). The 9 wt% rTE had smaller pore sizes, but not significantly different from native elastin (ANOVA, Tukey). The random orientation of fibers was confirmed for these electrospun samples (data not shown).

The cross-linked 15 wt% prTE had the same fiber structure as the uncross-linked rTE samples (Figure 4). Electrospun fibers that were not cross-linked and rinsed in PBS dissolved and lost their fiber structure, due to rTE's solubility in aqueous solutions. Cross-linking of 9 and 20 wt% rTE electrospun fibers also produced no visible alterations in fiber structure (data not shown).

Smooth muscle cell adhesion to adsorbed rTE

In the absence of serum, SMC adhesion to adsorbed rTE increased exponentially between rTE coating concentrations of 0.05 μ g/mL and 50 μ g/mL, where the number of adhered SMCs reached a plateau of 1.7×10^4 cells. There was no significant difference in the number of adhered SMCs for rTE coating concentrations between 50 μ g/mL and 5000 μ g/mL. Thus all subsequent adhesion studies were performed at the 50 μ g/mL adsorbed rTE coating concentration.

Adsorbed coatings of rTE, fibronectin, and collagen type I significantly increased SMC adhesion compared to uncoated tissue culture plastic (Figure 5).

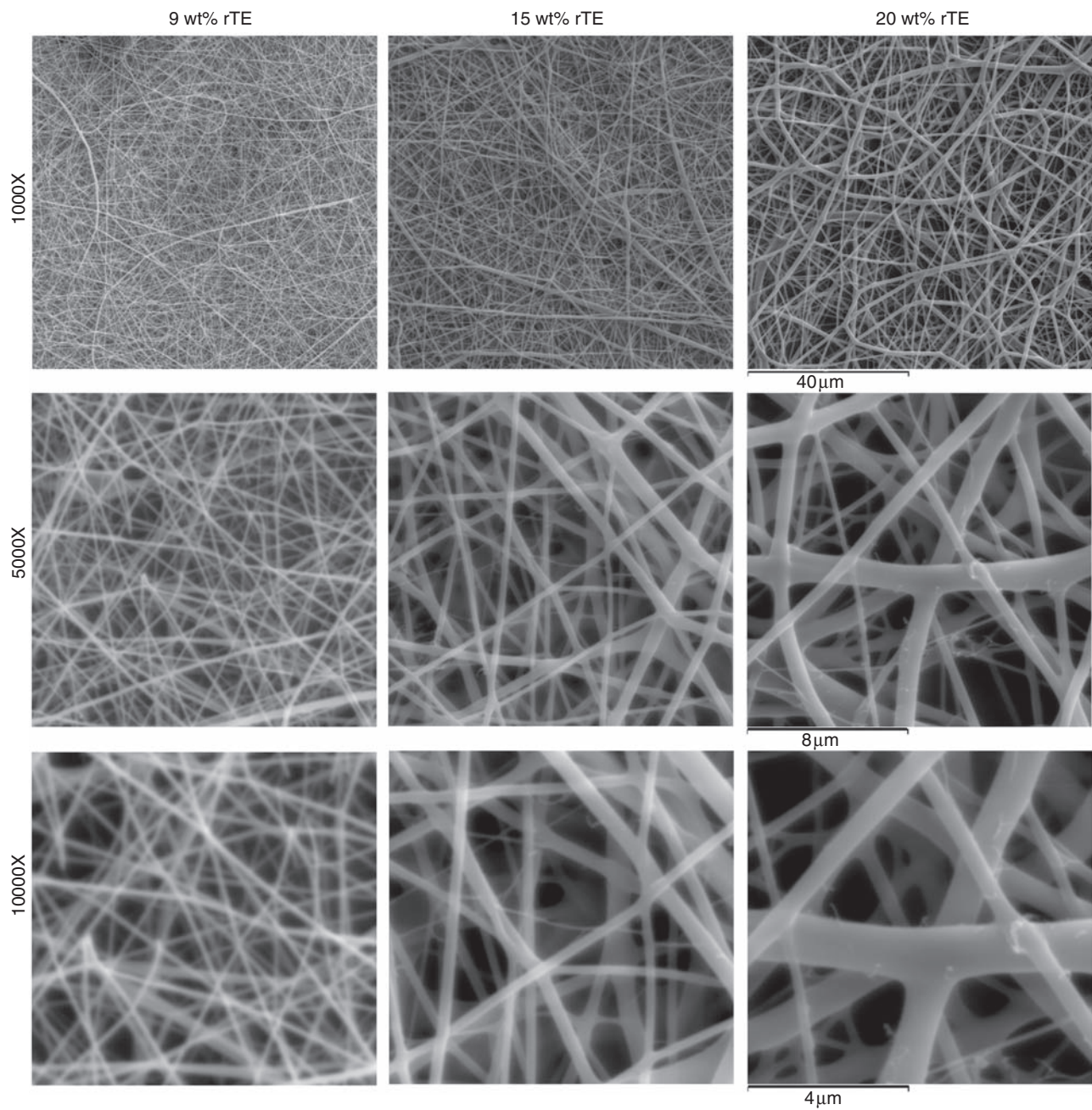


Figure 1. Comparison of electrospun rTE fibers from 9, 15, and 20 wt% solutions.

Note: The rTE fibers were randomly oriented. Fiber diameters were directly proportional to the concentration of the rTE solution. The electrospun rTE fibers from 9 and 15 wt% solutions had only round cross-sections, while isolated electrospun rTE fibers from 20 wt% solutions had flat cross-sections. SEM micrographs at magnifications of 1000 \times , 5000 \times , and 10,000 \times .

SMCs adhered to each of the protein coatings without significant differences between them. EDTA significantly reduced SMC adhesion to the adsorbed rTE and fibronectin coated wells, but had no effect on the collagen coated wells. The pertussis toxin and lactose had no significant effect on SMC adhesion to any of the tested surfaces.

Smooth muscle cell morphology and proliferation on electrospun prTE

SMCs adhered and proliferated on 9, 15 and 20 wt% electrospun prTE. Confocal images taken at 24 and 48 h showed cells spreading across the fibrous substrate and forming multiple attachment points to individual

15 wt% prTE fibers (Figure 6). These images also indicated an increase in cell concentration between 24 and 48 h post-seeding. Confocal images of SMCs on 9 and 20 wt% electrospun prTE confirmed similar responses in terms of cell attachment and spreading across the range of prTE fiber diameters (data not shown).

Growth curves were conducted using an alamarBlue® metabolic activity assay. The SMCs proliferated and were metabolically active on each of the four substrates (Figure 7). Logarithmic growth occurred between days 3 and 5 with growth reaching a plateau at day 5. Normalized alamarBlue® fluorescence values for day 5 were 1.82 ± 0.2 , 1.79 ± 0.2 , 1.88 ± 0.17 , and 1.73 ± 0.18 for electrospun prTE, coated prTE, Poly-D-Lysine glass, and TCP substrates, respectively. Doubling times were determined to be 84 ± 14 , 86 ± 3.6 , 72 ± 6.9 , and 78 ± 9.2 h for electrospun prTE, coated prTE, Poly-D-Lysine glass, and TCP substrates, respectively. There were no significant differences in doubling times between substrates (ANOVA).

A CyQUANT® assay was performed to quantify cell number on Day 8. Normalized cell numbers compared to TCP were $188 \pm 5.9\%$, $172 \pm 11.1\%$, and

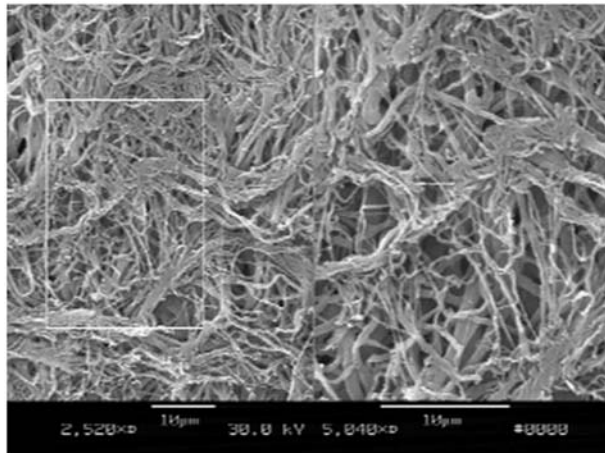


Figure 2. SEM micrograph of extracted native elastin from a porcine carotid artery.

Note: Scale bars indicate 10 μm .

$158 \pm 16.9\%$, for electrospun prTE, coated prTE, and Poly-D-Lysine glass, respectively. The cell numbers on each of the three substrates were significantly higher compared to the number of cells on TCP, but no differences were seen between electrospun prTE, coated prTE, and Poly-D-Lysine glass (ANOVA, Tukey *post hoc*, $p < 0.01$).

Discussion

Electrospinning was selected as the method to construct a reproducible, physiologically relevant human tropoelastin vascular medial biomaterial. Electrospinning of tropoelastin produced a vascular medial layer scaffold with highly controllable structural properties

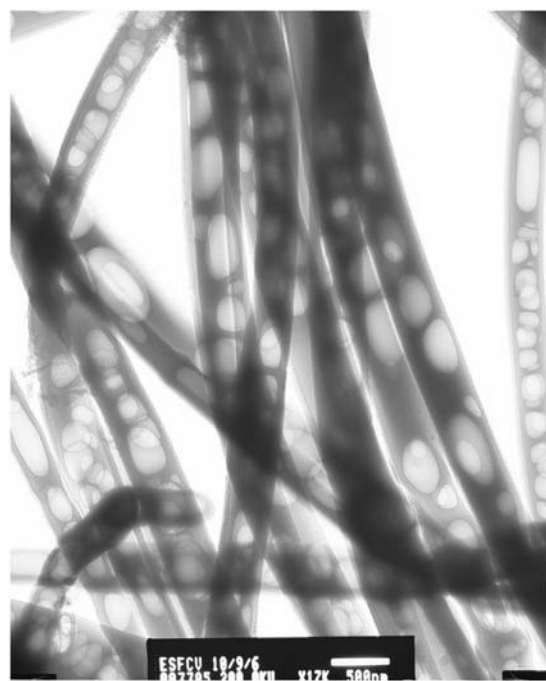


Figure 3. TEM micrograph of substructure of 15 wt% electrospun rTE fibers.

Note: Voids are visualized within the fibers. Scale bar indicates 500 nm.

Table 1. Fiber diameter and pore size for electrospun rTE and extracted porcine elastin.

Material	Fiber diameter Ave. \pm SD n = 20	Range of fiber diameters	Pore size Ave. \pm SD n = 10
Extracted porcine elastin	870 ± 450 nm	323–1843 nm	$3.7 \pm 1.6 \mu\text{m}^2$
9% electrospun rTE	167 ± 32 nm ^a	95–214 nm	$0.4 \pm 0.1 \mu\text{m}^2$
15% electrospun rTE (5 lots)	522 ± 67 nm ^a	261–1174 nm	$5.8 \pm 4.3 \mu\text{m}^2$
20% electrospun rTE	735 ± 270 nm	336–1430 nm	$4.9 \pm 2.4 \mu\text{m}^2$

^a $p < 0.01$, compared to extract porcine elastin.

comparable to the native extracellular matrix protein. The fiber and pore sizes of the prTE electrospun scaffolds were optimized to mimic the structural properties of native arterial elastin. Cross-linking using DSS enabled stabilization that prevented the fibers from dissolving in aqueous media without affecting the structural properties of the fiber. The electrospun prTE scaffolds were capable of supporting vascular SMC growth at rates comparable to coated-prTE and tissue culture plastic.

Electrospinning has advanced the tissue engineering field and proven to be a valuable tool to produce biomimetic scaffolds from both biodegradable polymers and natural proteins. The majority of current research has focused on the use of biodegradable polymers which lack the relevant cell signaling of natural matrix proteins. Elastin and collagen have been used to electrospin vascular grafts, yet these matrix proteins are frequently electrospun from solutions with fully cross-linked polymer fragments or from solutions containing a mixture of natural and synthetic polymers.^{12,34} Synthetic polymers such as poly(ethylene oxide) (PEO), poly(epsilon-caprolactone) (PCL), poly(lactic-co-glycolic acid) (PLGA), and polydioxanone (PDO) have been combined with protein blends (collagen, gelatin, and elastin) to electrospin scaffolds.^{24,25,34-38} Electrospinning of these blended solutions leads to an unknown amount, distribution, and structure of

protein within each individual fiber. Additionally, these scaffolds do not mimic the native arterial structure of separate elastin and collagen fibers and therefore are unlikely to support vascular cell functions. Li et al.²⁷ have electrospun calfskin type I collagen, bovine gelatin, extracted bovine α -elastin and are

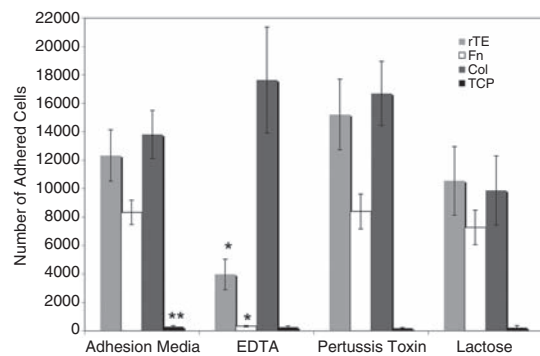


Figure 5. Characterization of the adhesion of SMCs to adsorbed rTE.

Note: SMCs were allowed to adhere to rTE, fibronectin (Fn), collagen type I (Col), or tissue culture treated plastic (TCP) in either adhesion media or adhesion media with a blocking reagent: EDTA, Pertussis toxin, or lactose. EDTA significantly reduced SMC adhesion to the rTE and Fn coated wells. * $p < 0.05$, compared to the same coating with adhesion media, ANOVA with a Tukey post hoc test.

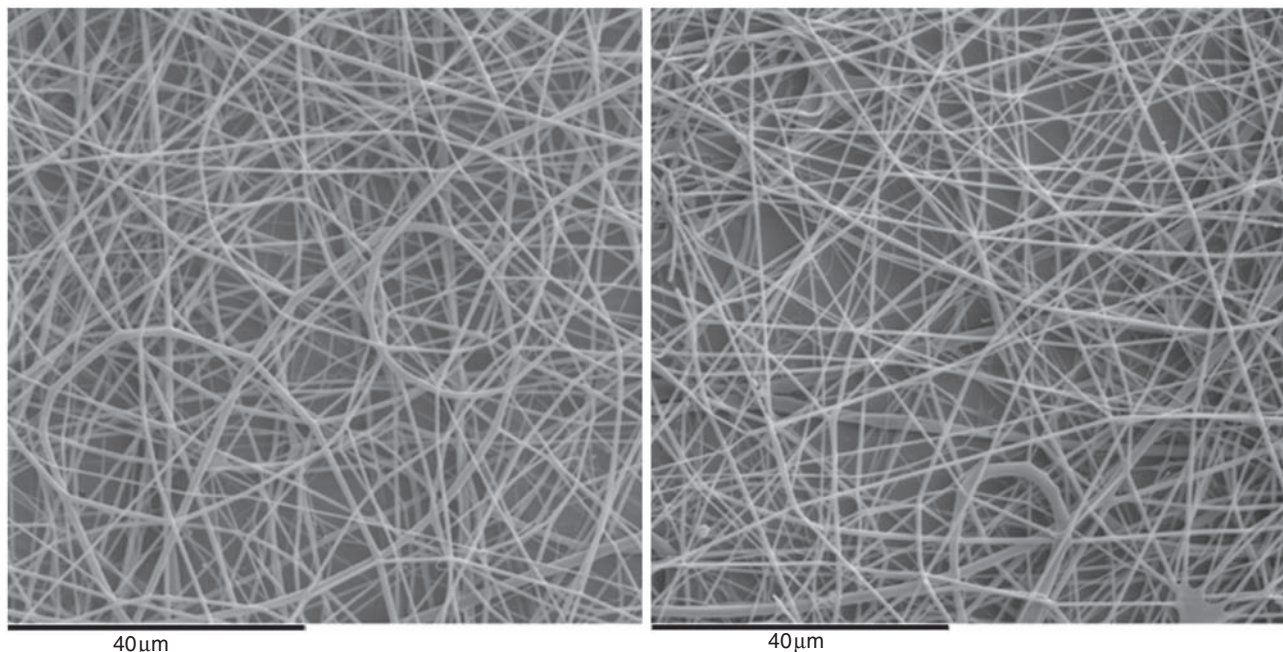


Figure 4. SEM micrograph of uncross-linked electrospun rTE (left) and cross-linked electrospun prTE (right) fibers produced from a 15 wt% rTE solution.

Note: No change in fiber structure was seen using the DSS cross-linker.

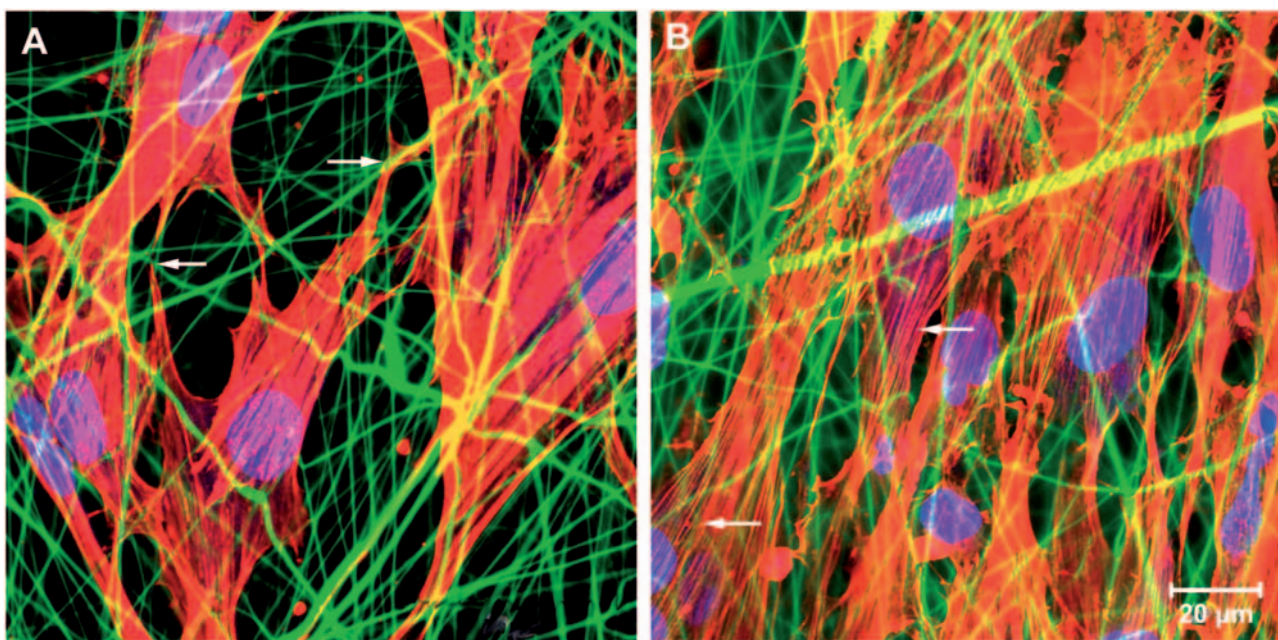


Figure 6. Morphology of SMCs seeded onto electrospun 15 wt% prTE for (A) 24 and (B) 48 h.

Note: Confocal images of prTE fibers (green) with actin cytoskeleton-phalloidin (red) and nuclei (blue) of SMCs. SMC pseudopodia made attachments to individual prTE fibers (arrows in A), SMC concentrations increased between 24 and 48 h, and SMCs formed actin stress fibers (arrows in B). Scale bar indicates 20 μ m.

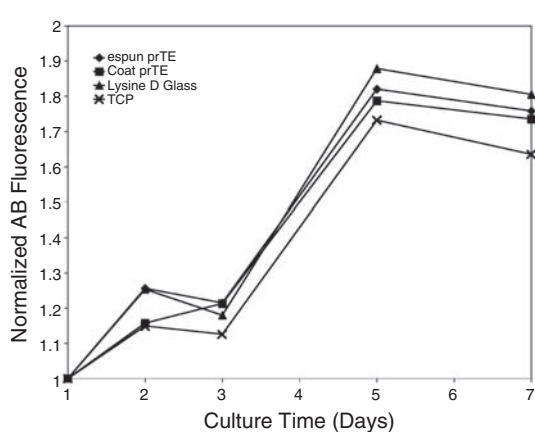


Figure 7. SMC proliferation on electrospun prTE, coated prTE, Poly-D-Lysine (Lysine D glass), and tissue culture plastic (TCP) over a 7 day time course.

Note: Cell metabolic activity was quantified using alamarBlue assay and the data normalized to the fluorescence reading at day 1. Data are the average of 3 lots of rTE solutions.

credited with the first published instance of human tropoelastin in HFP. The use of the elastin monomer, tropoelastin, provides an opportunity to control material properties and deliver solely 'elastin' fibers by cross-linking the final structure.

Optimizing the structure of the electrospun fibers requires balancing the fiber diameter, spacing, shape,

and orientation. Our 20 wt% rTE fibers had fiber diameters and pore sizes that matched the diameters of *in vivo* elastin fibers; yet their configuration of ribboned fibers differed from the cylindrical *in vivo* fibers. Similarly, using 20 wt% protein solutions and flow rates that ranged from 1 to 8 mL/h, electrospun bovine α -elastin and human tropoelastin fibers were 'ribbon-like' in appearance, with ribbon widths ranging from 0.6 to 3.6 μ m and 1.4 to 7.4 μ m.²⁷ This ribboning phenomenon was seen in the larger spun fibers of our electrospun 20 wt% rTE fibers. The ribboning results as the bulk material and solvent separated during fiber formation,³⁹ followed by the subsequent collapsing of fibers forming the flattened ribbons. Additionally, the 20 wt% human tropoelastin fibers from Li et al. had average fiber diameters of approximately 2.2 μ m,²⁷ which was significantly greater than our average diameter of 735 nm for a flow rate of 2 mL/h. This was likely due to differences in their electrospinning parameters, most notably a lower accelerating voltage of 10 kV versus 18.5 kV and a larger gap distance of 14 cm versus 12.5 cm, as well as the variability induced by the measurement of the larger dimension (width vs. thickness) of the ribboned fiber. Due to the ribboned-structure in our 20 wt% rTE scaffolds, the 15 wt% rTE solutions were used for all subsequent studies. Using 15 wt% rTE solutions, we were able to produce cylindrical prTE fibers (Figure 1), a structure similar to native medial elastin structure.

Using monomer protein solutions necessitates the use of cross-linking to stabilize the electrospun fibers. The monomer tropoelastin is soluble in aqueous solutions and would therefore lose its macro fiber structure upon introduction to aqueous media. This cross-linking has a significant effect on the structural properties of the electrospun materials⁴⁰ and can lead to complications of calcification and cytotoxicity. This is the first reported use of DSS to cross-link tropoelastin electrospun materials. DSS was selected to cross-link the rTE due to the low reported cytotoxicity of its aqueous equivalent bis(sulfosuccinimidyl) suberate (BS³) and its ability to react with amine groups on lysine residues of adjacent molecules to form amide bond cross-links.^{41–43} The prTE was cross-linked with DSS in anhydrous ethyl acetate at a concentration sufficient to attain 100% cross-linking based upon a molecular weight of 62,500 and 35 lysines per molecule. Monomeric rTE maintains its fiber structure in ethyl acetate giving the DSS cross-linker time to stabilize or lock the fiber structure in place. Use of high concentrations of cross-linker can lead to blocking of amine groups resulting in fewer cross-links being formed. DSS forms an 8-atom bridge (11.4 Å) between tropoelastin monomers to form polytropoelastin, and has proven to be an effective method for cross-linking rTE electrospun materials. Electrospun tropoelastin alone or elastin with collagen have previously been cross-linked with glutaraldehyde vapor,^{29,34} hexamethylene diisocyanate (HMDI),^{27,44} or BS³.^{41,43,45} The glutaraldehyde vapor caused melting of the collagen/elastin fibers³⁴ and may lead to calcification of the fibers and a cytotoxic environment. HMDI binds lysine or hydroxylysine residues and has been used primarily with collagen biomaterials (e.g. Permacol, Covidien). BS³ uses the same mechanism of cross-linking as DSS. Thus DSS, HMDI, and BS³ are promising as cross-linkers of protein monomers but their full biological effects on cell proliferation, mechanical properties, and host reactions are unknown. The proliferation of SMCs on the DSS cross-linked prTE supports the cytocompatibility of the DSS crosslinker. The mechanical properties and host reactions will depend on the concentration of the electrospinning solution, as well as the configuration of the final biomaterial as a flat or tubular scaffold. For vascular applications, the appropriate mechanical evaluations (e.g., burst pressure, compliance) of DSS-cross-linked prTE in the tubular configuration should be determined.

Support of vascular cell adhesion and growth is required for tissue-engineered scaffolds. Elastin is an important regulator of SMC phenotype. Karnik et al. demonstrated an increase in vascular SMC proliferation rates in cells unable to synthesize elastin.⁴⁶ Yet the addition of exogenous tropoelastin to the

growth culture recovered normal proliferation rates, equivalent to wild type cells.⁴⁶ It has been suggested that elastin (as a signaling molecule) activates the G-protein coupled pathway that ultimately leads to Rho-induced actin polymerization in vascular SMCs.⁴⁷ Our study, where pertussis toxin was unable to block adhesion, suggests that the G-protein coupled pathway does not play a role in the initial cell adhesion to rTE. There have been several elastin binding proteins (EBP) identified, including a 67-kDa protein that is also identified as a galactoside-binding lectin,^{48–51} a 120-kDa protein (elastonectin) and a 59-kDa VGVAPG-binding protein.⁵² These EBPs act as chaperones during elastin assembly by preventing intracellular aggregation of tropoelastin as well as protecting tropoelastin and mature elastin from proteolysis. EBP binds elastin through the VGVAPG motif within exon 24⁵³ and signaling through this receptor may influence SMC proliferation and differentiation.⁴⁷ Fetal bovine chondrocyte adhesion was associated with the COOH terminus of tropoelastin and dependent on glycosaminoglycans, while integrin and EBP inhibitors had no effect on chondrocyte adhesion and spreading on the COOH terminus of tropoelastin.⁵³ Thus, the EBPs do not appear to play a role in cell adhesion to tropoelastin, which was confirmed in this study with the inability of lactose to block SMC adhesion to rTE. A direct link between cell adhesion to tropoelastin and the $\alpha_v\beta_3$ integrin has been demonstrated with human dermal fibroblasts.⁵⁴ Similarly, in this current study the adsorbed rTE, as well as the adsorbed fibronectin, supported SMC adhesion through cationic binding, which was blocked by EDTA. This integrin-mediated adhesion is likely due to $\alpha_v\beta_3$ integrin interaction with GRKRK motif.⁵⁴ Differences in cell binding mechanisms to tropoelastin are likely due to the utilization of different cell types.

Coatings of rTE can be used to modify devices such as stents and vascular graft materials. Optimal cell adhesion occurred on substrates coated with 50 µg/mL or greater and consequently, this value can be used as the baseline value for designing rTE modified surfaces. The three-dimensional electrospun prTE supported SMC proliferation indicating the cytocompatibility of the DSS-cross-linked prTE. SMC metabolic activity (as indicated by the alamarBlue® assay) on electrospun prTE increased between day 1 and day 7 similar to the activity of SMCs on coated prTE, Poly-D-Lysine, and TCP. While the alamarBlue® assay does not quantify exact cell numbers, rather cell metabolic activity, it is correlated to the growth rates of cells in culture. After 8 days of growth, the cellular DNA content on the electrospun prTE, coated prTE, and Poly-D-Lysine (CyQUANT® assay) were equivalent and greater than the DNA content

on TCP. The ability of electrospun tropoelastin to support cell growth agrees with the results of Li et al., who demonstrated human embryonic palatal mesenchymal cell (HEPM) growth on both electrospun elastin and tropoelastin.²⁷ Similar to the HEPM cells, SMCs formed distinct organized cytoskeletal fibers with multiple pseudopodia attachments to the prTE fibers. Likewise, human dermal fibroblasts attached and proliferated on electrospun tropoelastin.²⁹ Though a direct comparison is difficult to make due to differences in study conditions, our SMC growth data was similar to Karnik's data for wild-type SMCs, which demonstrated a 2-fold increase in cell numbers at 72 h.⁴⁶ Modest cell growth rates, the presence of distinct stress fibers, and multiple attachment points on each of the three biomaterials of prTE tested suggests that SMCs grown on prTE adopt a contractile phenotype, which could ultimately provide physiologic vascular compliance and vasomotor tone. Further investigation into the three-dimensional growth patterns of SMCs on electrospun prTE and their remodeling effect on the protein scaffold in long-term cultures is warranted.

Conclusion

In conclusion, an electrospun cross-linked rTE vascular scaffold material has been developed. This novel tissue engineered scaffold has structural properties similar to native elastin within the medial layers of elastic arteries. The diameter, length, fiber size, and fiber spacing of the electrospun prTE scaffold were easily manipulated providing a high degree of control for tissue engineering. The electrospun prTE biomaterial supported SMC attachment (via an integrin-mediated pathway), spreading, and growth. A cross-linked stable polymer produced from rTE, which matched the structure of medial elastin, may provide the optimal environment needed for a functional tissue-engineered scaffold. The development of this technology provides a tool for tissue engineers, which can ultimately lead to natural protein-based vascular grafts.

Acknowledgements

We would like to thank Dr. Jack M. McCarthy for his assistance with SEM and TEM imaging, Dr. Brian Kim for his assistance with cross-linking modalities, and Dr. Sean Kirkpatrick for his assistance in evaluating fiber orientation. Tropoelastin was produced with the excellent technical assistance of Amy Jay, Cher Hawkey, and Rose Merten. This work was funded in part by the NIH R01-HL095474 and Department of the Army, Grant Nos. W81XWH-04-1-0841 and W81XWH-05-1-0586. This work does not necessarily reflect the policy of the government and no official endorsement should be inferred.

References

- Lloyd-Jones D, Adams RJ, Brown TM, Carnethon M, Dai S, De Simone G, et al. Heart disease and stroke statistics—2010 update: a report from the American Heart Association. *Circulation* 2009; 121: e46–e215.
- Brewster DC. Prosthetic grafts. In: Rutherford RB (ed.) *Vascular surgery*, 4th ed. Philadelphia: W.B.Saunders, 1995, pp.492–521.
- Abbott WM and Rehring TF. Biologic and synthetic prosthetic materials for vascular conduits. In: Hobson RW, Wilson S, Veith FJ (eds) *Vascular surgery: principles and practice*, 3rd ed. New York: Marcel Dekker, 2004, pp.611–620.
- Sawyer PN, Fitzgerald J, Kaplitt MJ, Sanders RJ, Williams GM, Leather RP, et al. Ten year experience with the negatively charged glutaraldehyde-tanned vascular graft in peripheral vascular surgery. Initial multicenter trial. *Am J Surg* 1987; 154: 533–537.
- Dardik H, Wengerter K, Qin F, Pangilinan A, Silvestri F, Wolodiger F, et al. Comparative decades of experience with glutaraldehyde-tanned human umbilical cord vein graft for lower limb revascularization: an analysis of 1275 cases. *J Vasc Surg* 2002; 35: 64–71.
- Strobel R, Boontje AH and Van Den Dungen JJ. Aneurysm formation in modified human umbilical vein grafts. *Eur J Vasc Endovasc Surg* 1996; 11: 417–420.
- Gui L, Muto A, Chan SA, Breuer CK and Niklason LE. Development of decellularized human umbilical arteries as small-diameter vascular grafts. *Tissue Eng Part A* 2009; 15: 2665–2676.
- L'Heureux N, Dusserre N, Marini A, Garrido S, de la Fuente L and McAllister T. Technology insight: the evolution of tissue-engineered vascular grafts—from research to clinical practice. *Nat Clin Pract Cardiovasc Med* 2007; 4: 389–395.
- McAllister TN, Maruszewski M, Garrido SA, Wystrychowski W, Dusserre N, Marini A, et al. Effectiveness of haemodialysis access with an autologous tissue-engineered vascular graft: a multicentre cohort study. *Lancet* 2009; 373: 1440–1446.
- Megelski S, Stephens JS, Chase DB and Rabolt JF. Micro and nano-structured surface morphology on electrospun polymer fibers. *Macromolecules* 2002; 35: 8456–8466.
- Murugan R and Ramakrishna S. Nano-featured scaffolds for tissue engineering: a review of spinning methodologies. *Tissue Eng* 2006; 12: 435–447.
- Boland ED, Matthews JA, Pawlowski KJ, Simpson DG, Wnek GE and Bowlin GL. Electrospinning collagen and elastin: preliminary vascular tissue engineering. *Front Biosci* 2004; 9: 1422–1432.
- Roach MR and Burton AC. The reason for the shape of the distensibility curves of arteries. *Can J Biochem Physiol* 1957; 35: 681–690.
- Baxter BT, McGee GS, Shively VP, Drummond IA, Dixit SN, Yamauchi M, et al. Elastin content, cross-links, and mRNA in normal and aneurysmal human aorta. *J Vasc Surg* 1992; 16: 192–200.

15. Curran ME, Atkinson DL, Ewart AK, Morris CA, Leppert MF and Keating MT. The elastin gene is disrupted by a translocation associated with supravalvular aortic stenosis. *Cell* 1993; 73: 159–168.
16. Ewart AK, Jin W, Atkinson D, Morris CA and Keating MT. Supravalvular aortic stenosis associated with a deletion disrupting the elastin gene. *J Clin Invest* 1994; 93: 1071–1077.
17. Gandhi RH, Irizarry E, Cantor JO, Keller S, Nackman GB, Halpern VJ, et al. Analysis of elastin cross-linking and the connective tissue matrix of abdominal aortic aneurysms. *Surgery* 1994; 115: 617–620.
18. Li DY, Toland AE, Boak BB, Atkinson DL, Ensing GJ, Morris CA, et al. Elastin point mutations cause an obstructive vascular disease, supravalvular aortic stenosis. *Hum Mol Genet* 1997; 6: 1021–1028.
19. Rizzo RJ, McCarthy WJ, Dixit SN, Lilly MP, Shively VP, Flinn WR, et al. Collagen types and matrix protein content in human abdominal aortic aneurysms. *J Vasc Surg* 1989; 10: 365–373.
20. Urban Z, Michels VV, Thibodeau SN, Donis-Keller H, Csiszar K and Boyd CD. Supravalvular aortic stenosis: a splice site mutation within the elastin gene results in reduced expression of two aberrantly spliced transcripts. *Hum Genet* 1999; 104: 135–142.
21. Daamen WF, Veerkamp JH, van Hest JC and van Kuppevelt TH. Elastin as a biomaterial for tissue engineering. *Biomaterials* 2007; 28: 4378–4398.
22. Patel A, Fine B, Sandig M and Mequanint K. Elastin biosynthesis: The missing link in tissue-engineered blood vessels. *Cardiovasc Res* 2006; 71: 40–49.
23. Buttafoco L, Kolkman NG, Poot AA, Dijkstra PJ, Vermes I and Feijen J. Electrospinning collagen and elastin for tissue engineering small diameter blood vessels. *J Control Release* 2005; 101: 322–324.
24. Buttafoco L, Kolkman NG, Engbers-Buijtenhuijs P, Poot AA, Dijkstra PJ, Vermes I, et al. Electrospinning of collagen and elastin for tissue engineering applications. *Biomaterials* 2006; 27: 724–734.
25. Lee SJ, Yoo JJ, Lim GJ, Atala A and Stitzel J. In vitro evaluation of electrospun nanofiber scaffolds for vascular graft application. *J Biomed Mater Res A* 2007; 83: 999–1008.
26. Li M, Mondrinos MJ, Chen X, Gandhi MR, Ko FK and Lelkes PI. Co-electrospun poly(lactide-co-glycolide), gelatin, and elastin blends for tissue engineering scaffolds. *J Biomed Mater Res A* 2006; 79: 963–973.
27. Li M, Mondrinos MJ, Gandhi MR, Ko FK, Weiss AS and Lelkes PI. Electrospun protein fibers as matrices for tissue engineering. *Biomaterials* 2005; 26: 5999–6008.
28. Stitzel J, Liu J, Lee SJ, Komura M, Berry J, Soker S, et al. Controlled fabrication of a biological vascular substitute. *Biomaterials* 2006; 27: 1088–1094.
29. Rnjak J, Li Z, Maitz PK, Wise SG and Weiss AS. Primary human dermal fibroblast interactions with open weave three-dimensional scaffolds prepared from synthetic human elastin. *Biomaterials* 2009; 30: 6469–6477.
30. Lowry O, Gilligan D and Katersky E. The determination of collagen and elastin in tissues, with results obtained in various normal tissues from different species. *J Biol Chem* 1941; 139: 795–804.
31. Lansing A, Rosenthal T, Alex M and Dempsey E. The structure and chemical characterization of elastic fibers as revealed by elastase and by electron microscopy. *Anat Rec* 1952; 114: 555–575.
32. Vartanian KB, Kirkpatrick SJ, Hanson SR and Hinds MT. Endothelial cell cytoskeletal alignment independent of fluid shear stress on micropatterned surfaces. *Biochem Biophys Res Commun* 2008; 371: 787–792.
33. Stegemann JP and Nerem RM. Phenotype modulation in vascular tissue engineering using biochemical and mechanical stimulation. *Ann Biomed Eng* 2003; 31: 391–402.
34. Heydarkhan-Hagvall S, Schenke-Layland K, Dhanasopon AP, Rofail F, Smith H, Wu BM, et al. Three-dimensional electrospun ECM-based hybrid scaffolds for cardiovascular tissue engineering. *Biomaterials* 2008; 29: 2907–2914.
35. Smith MJ, McClure MJ, Sell SA, Barnes CP, Walpeth BH, Simpson DG, et al. Suture-reinforced electrospun polydioxanone-elastin small-diameter tubes for use in vascular tissue engineering: a feasibility study. *Acta Biomater* 2008; 4: 58–66.
36. Smith MJ, White Jr KL, Smith DC and Bowlin GL. In vitro evaluations of innate and acquired immune responses to electrospun polydioxanone-elastin blends. *Biomaterials* 2009; 30: 149–159.
37. Thomas V, Zhang X, Catledge SA and Vohra YK. Functionally graded electrospun scaffolds with tunable mechanical properties for vascular tissue regeneration. *Biomed Mater* 2007; 2: 224–232.
38. Zhang X, Thomas V, Xu Y, Bellis SL and Vohra YK. An in vitro regenerated functional human endothelium on a nanofibrous electrospun scaffold. *Biomaterials* 2010; 31: 4376–4381.
39. Koombhongse S, Liu W and Reneker DH. Flat polymer ribbons and other shapes by electrospinning. *J Polym Sci Pol Phys* 2001; 39: 2598–2606.
40. Zeugolis DI, Paul GR and Attenburrow G. Cross-linking of extruded collagen fibers—a biomimetic three-dimensional scaffold for tissue engineering applications. *J Biomed Mater Res A* 2009; 89: 895–908.
41. Mithieux SM, Rasko JE and Weiss AS. Synthetic elastin hydrogels derived from massive elastic assemblies of self-organized human protein monomers. *Biomaterials* 2004; 25: 4921–4927.
42. Mithieux SM, Wise SG, Raftery MJ, Starcher B and Weiss AS. A model two-component system for studying the architecture of elastin assembly in vitro. *J Struct Biol* 2005; 149: 282–289.
43. Wise SG, Mithieux SM, Raftery MJ and Weiss AS. Specificity in the coacervation of tropoelastin: solvent exposed lysines. *J Struct Biol* 2005; 149: 273–281.
44. Nivison-Smith L, Rnjak J and Weiss AS. Synthetic human elastin microfibers: stable cross-linked

- tropoelastin and cell interactive constructs for tissue engineering applications. *Acta Biomater* 2010; 6: 354–359.
45. Dyksterhuis LB, Baldeck C, Lammie D, Wess TJ and Weiss AS. Domains 17-27 of tropoelastin contain key regions of contact for coacervation and contain an unusual turn-containing crosslinking domain. *Matrix Biol* 2007; 26: 125–135.
 46. Karnik SK, Brooke BS, Bayes-Genis A, Sorensen L, Wythe JD, Schwartz RS, et al. A critical role for elastin signaling in vascular morphogenesis and disease. *Development* 2003; 130: 411–423.
 47. Karnik SK, Wythe JD, Sorensen L, Brooke BS, Urness LD and Li DY. Elastin induces myofibrillogenesis via a specific domain, VGVAPG. *Matrix Biol* 2003; 22: 409–425.
 48. Hinek A, Wrenn DS, Mecham RP and Barondes SH. The elastin receptor: a galactoside-binding protein. *Science* 1988; 239: 1539–1541.
 49. Hinek A, Rabinovitch M, Keeley F, Okamura-Oho Y and Callahan J. The 67-kD elastin/laminin-binding protein is related to an enzymatically inactive, alternatively spliced form of beta-galactosidase. *J Clin Invest* 1993; 91: 1198–1205.
 50. Mecham RP, Hinek A, Entwistle R, Wrenn DS, Griffin GL and Senior RM. Elastin binds to a multifunctional 67-kilodalton peripheral membrane protein. *Biochemistry* 1989; 28: 3716–3722.
 51. Robert L, Jacob MP, Fulop T, Timar J and Hornebeck W. Elastonectin and the elastin receptor. *Pathol Biol (Paris)* 1989; 37: 736–741.
 52. Blood CH, Sasse J, Brodt P and Zetter BR. Identification of a tumor cell receptor for VGVAPG, an elastin-derived chemotactic peptide. *J Cell Biol* 1988; 107: 1987–1993.
 53. Broekelmann TJ, Kozel BA, Ishibashi H, Werneck CC, Keeley FW, Zhang L, et al. Tropoelastin interacts with cell-surface glycosaminoglycans via its COOH-terminal domain. *J Biol Chem* 2005; 280: 40939–40947.
 54. Bax DV, Rodgers UR, Bilek MM and Weiss AS. Cell adhesion to tropoelastin is mediated via the C-terminal GRKRK motif and integrin alphaVbeta3. *J Biol Chem* 2009; 284: 28616–28623.